November 1994

Mössbauer, magnetic, and electronic-structure studies of $YFe_{12-x}Mo_x$ compounds

I.A. Al-Omari
University of Nebraska - Lincoln

Sitaram Jaswal
University of Nebraska, sjaswal1@unl.edu

A.S. Fernando
University of Nebraska - Lincoln

David J. Sellmyer
University of Nebraska-Lincoln, dsellmyer@unl.edu

H.H. Hamdeh
Department of Physics, Wichita State University, Wichita, Kansas

Mössbauer, magnetic, and electronic-structure studies of $YFe_{12-x}Mo_x$ compounds

I. A. Al-Omari, S. S. Jaswal, A. S. Fernando, and D. J. Sellmyer
Behlen Laboratory of Physics and Center for Materials Research and Analysis, University of Nebraska, Lincoln, Nebraska 68588-0111

H. H. Hamdeh
Department of Physics, Wichita State University, Wichita, Kansas 67260
(Received 26 May 1994)

Mössbauer spectra, magnetization measurements, and self-consistent spin-polarized electronic structures of $YFe_{12-x}Mo_x$, where $x=0.5$, 1.0, 2.0, 3.0, and 4.0, are reported. The ternary compounds $YFe_{12-x}Mo_x$ have the crystalline tetragonal $ThMn_{12}$ structure. Analyses of the Mössbauer spectra show that Mo atoms occupy the 8*i* Fe sites of the $ThMn_{12}$ structure, in agreement with previous observations. Room-temperature magnetic and Mössbauer measurements show that the compounds with $x \leq 2.0$ are ferromagnetic and with $x \geq 3.0$ are paramagnetic. Measurements at 25 K show that all the samples are magnetically ordered. The magnetic hyperfine field is found to decrease with increasing Mo concentration, which is in qualitative agreement with the calculated magnetic moments. The calculated magnetization decreases less rapidly with increasing x than the experimental data. In general the data suggest that with increasing Mo concentration there is an increase of antiferromagnetic coupling among the Fe moments, which leads to cluster-glass or spin-glass-like phenomena. The measured isomer shift relative to α-iron is found to decrease linearly with x.

I. INTRODUCTION

A good permanent magnet requires a relatively high Curie temperature, large saturation magnetization, and large uniaxial anisotropy. Intermetallic compounds of the type $RFe_{12-x}M_x$ (R = Gd, Y, Nd, and Sm; M = Ti, V, Cr, Mo, W, and Si) have been the subject of many recent x-ray-diffraction,[1-3] neutron-diffraction,[4,5] electronic-structure,[6-9] Mössbauer spectroscopy,[10-17,23,24] and magnetism investigations[1,3,4,18-24] due to their potential as permanent magnets. X-ray diffraction on powder samples showed that these compounds crystallize in the body-centered-tetragonal $ThMn_{12}$ structure. The metal M is used to stabilize the otherwise instable RFe_{12} compound. X-ray diffraction,[1] neutron diffraction,[4] and Mössbauer spectroscopy[10-12,24] show that M atoms substitute for the 8*i* site of the iron in the $ThMn_{12}$ structure.

In this paper we explore the effect of the stabilizing element Mo on the electronic structure and magnetic properties of Fe-rich $YFe_{12-x}Mo_x$ for $x=0.5$, 1, 2, 3, and 4. Electronic-structure calculations are used to derive partial density of states and local magnetic moments. Mössbauer and magnetic measurements are used to find hyperfine fields (H_{hf}), site occupation, isomer shifts (δ), and magnetization (M).

II. ELECTRONIC-STRUCTURE CALCULATIONS

$YFe_{12-x}Mo_x$ has the $ThMn_{12}$ structure which is body-centered tetragonal (space group $I4/mmm$) with the Fe atoms occupying 8*f*, 8*i*, and 8*j* sites. The stabilizing Mo atoms substitute randomly for the 8*i* Fe atoms. The disordered alloy is simulated by a supercell containing four primitive cells of $ThMn_{12}$ structure. The tetragonal cell has dimensions of a, a, $2c$, and contains 52 atoms. The calculations reported in Ref. 8 are for the ordered hypothetical $YFe_{12-x}Mo_x$ structures with $x=1$, 2, 3, and 4.

The self-consistent spin-polarized electronic-structure calculations are based on the linear-muffin-tin-orbitals method in the scalar-relativistic and local-density approximations. The core states for the constituent atoms were frozen to be the same as the atomic states found self-consistently. The *s*, *p*, and *d* orbitals were used for the valence states of each atom. The Hamiltonian and overlap matrices are 468×468. The ratio of the Wigner-Sitez radii used are $r_Y : r_{Fe} : r_{Mo} = 1.35 : 1 : 1.12$. The calculations were performed for six k points in the irreducible part of the Brillouin zone.

III. EXPERIMENTAL METHODS

The fabrication of the compounds $YFe_{12-x}Mo_x$ is described in previous papers.[7,19] The samples for Mössbauer spectroscopy were prepared by sprinkling a thin layer of the powder material on a piece of tape. The samples were studied by using the transmission mode of Fe^{57} Mössbauer spectroscopy at room temperature and at low temperature. The velocity drive operates in the constant acceleration mode. The γ-ray source was Co^{57} in Pd. The isomer shifts were measured relative to α-iron at room temperature (RT). The low-temperature spectra were obtained using a closed-cycle cryostat. The magnetization and coercivity were measured by alternating gradient force magnetometer (AGFM) and superconducting quantum interference device (SQUID). The spectra were fitted by a standard fitting program, with different subspectra for each spectrum. The intensities of the subspectra were calculated according to previous models by Den-

TABLE I. Intensities (%) for the different ferromagnetic subspectra of $YFe_{12-x}Mo_x$ compounds after renormalization.

Iron site	YFe_8Mo_4	YFe_9Mo_3	$YFe_{10}Mo_2$	$YFe_{11}Mo$	$YFe_{11.5}Mo_{0.5}$
8*i* 13 Fe NN		0.0	0.0	7.4	15.8
12 Fe NN		0.0	3.3	12.4	11.4
11 Fe NN		0.0	6.7	28.	3.3
10 Fe NN		0.0	6.7	0.0	0.0
9 Fe NN		11.0	3.3	0.0	0.0
8 Fe NN		0.0	0.0	0.0	0.0
8*j* or 8*f*	50.0				
10 Fe NN		0.0	0.0	12.0	22.1
9 Fe NN		0.0	11.4	16.0	12.6
8 Fe NN		10.0	17.2	8.0	0.0
7 Fe NN		19.7	11.4	0.0	0.0
6 Fe NN		14.8	0.0	0.0	0.0

nissen, Coehoorn, and Buschow[10] and Sinnemann, Rosenberg, and Buschow[11] for similar compounds with the $ThMn_{12}$ structure. By assuming that the Mo goes randomly to the 8*i* site of the three iron sites, the probability $P(n,m,y)$ of finding m Mo atoms in a shell of n nearest-neighbor 8*i* atoms is given by the binomial distribution function

$$P(n,m,y)=[n!/m!(n-m)!]y^m(1-y)^{n-m},$$

where y is the relative atomic fraction of the Mo atoms occupying the 8*i* sites. On the basis of these probabilities the subspectra with intensities less than 3% were neglected and the remaining intensities were renormalized with the final results shown in Table I for different concentrations (x) of Mo.

IV. RESULTS AND DISCUSSION

A. Electronic structure

The spin-polarized partial densities of states (DOS) are shown in Figs. 1–4 for $x=1-4$, respectively. The results for $x=1$ are compared with photoemission data in Ref. 7. As expected, DOS are dominated by Fe *d* states near the Fermi level but the Mo contribution increases with increasing x. The Fe magnetic moments decrease with increasing x as shown in Table II in spite of the lattice expansion. This is due to a strong hybridization of the Fe and Mo *d* bands. The Curie temperature decreases with increasing x for the same reason. The calculated moments are in good agreement with neutron-scattering data for $YFe_{11}Mo$ in Ref. 5. The early transition elements Y and Mo develop negative moments due to interatomic exchange interactions and these moments also decrease in magnitude with increasing x. Our moment results for $x=4$ are similar to those of Coehoorn[6] except for the 8*j* site where his value is considerably lower than ours. The calculated values of magnetization per formula unit are also compared with the experimental data in Table II. The calculations predict the system to be ferromagnetic for all four values of x. The experimental magnetization decreases more rapidly with increasing x than the calculated result. In fact, Sun *et al.*[19] report the

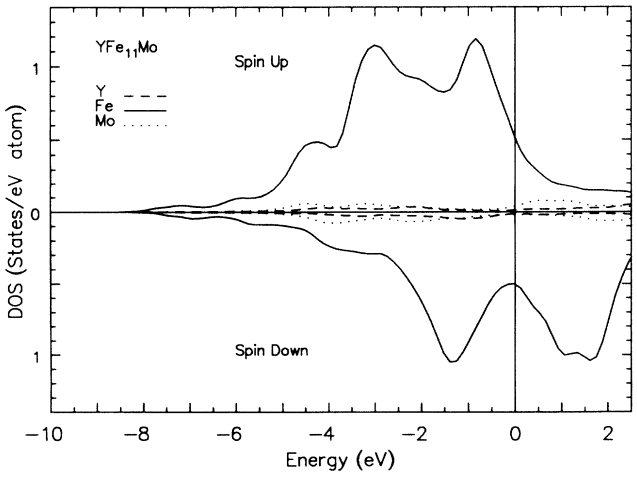

FIG. 1. Spin-polarized partial density of states for $YFe_{11}Mo$.

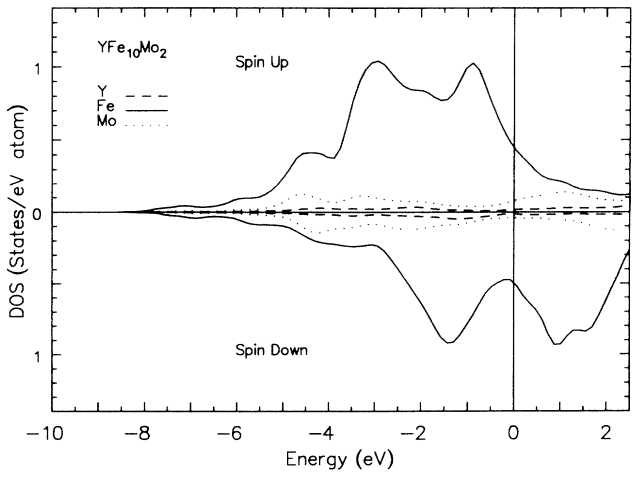

FIG. 2. Spin-polarized partial density of states for $YFe_{10}Mo_2$.

TABLE II. Local average magnetic moments (μ) in μ_B and total magnetization per formula unit (μ_B/f.u.) in $YFe_{12-x}Mo_x$.

	Local average moments					Magnetization	
x	Y(a)	Mo(i)	Fe(i)	Fe(j)	Fe(f)	Theory	Expt.
1	−0.37	−0.66	2.46	2.11	1.55	21.1	23.7[a]
1[b]		−1.00	2.43(55)	2.42(64)	2.15(45)		
2	−0.37	−0.53	2.28	2.01	1.62	17.7	14.2[a]
3	−0.32	−0.42	2.03	1.89	1.50	14.0	3.6[a]
4	−0.27	−0.28		1.76	1.30	10.8	1.7[a]
4[c]	−0.18	−0.23		1.40	1.23	8.9	

[a]SQUID measurements at 5 K and 50 kOe (magnetization was saturated for $x=1$ and 2 but not for $x=3$ and 4).
[b]Neutron-scattering results of Ref. 5.
[c]Reference 6.

system to be paramagnetic for $x=4$. The origin of the disagreement between the calculated and experimental magnetization with increasing x may be due to the noncollinear ordering of magnetic moments which is not considered in the present calculations.

B. Mössbauer and magnetic data

Figure 5 shows the Mössbauer spectra and the fitting of $YFe_{12-x}Mo_x$ with $x=0.5$, 1, and 2 at $T=295$ K. All the spectra show a magnetic ordering with different magnetic hyperfine fields. These results are similar to those of Ref. 24. The average hyperfine field ($\bar{H}_{hf}$) was found to decrease with increasing Mo concentration as seen in Fig. 6, which is in qualitative agreement with the magnetization measurements by Sun *et al.*[19] Previous Mössbauer measurements for $YFe_{10}Mo_2$ at $T=10$ K by Denissen, Coehoorn, and Buschow[10] showed that the $\bar{H}_{hf}$ decrease in the order of the sites 8i, 8j, and 8f. In our analysis we found the same order for $\bar{H}_{hf}$ which is in agreement with our calculated magnetic moments.

The average isomer shift ($\bar{\delta}$) was found to decrease linearly with x as shown in Fig. 7 and the $T=295$ K data were fitted by a least-squares method (solid line) with the fitting parameters given by the following equation:

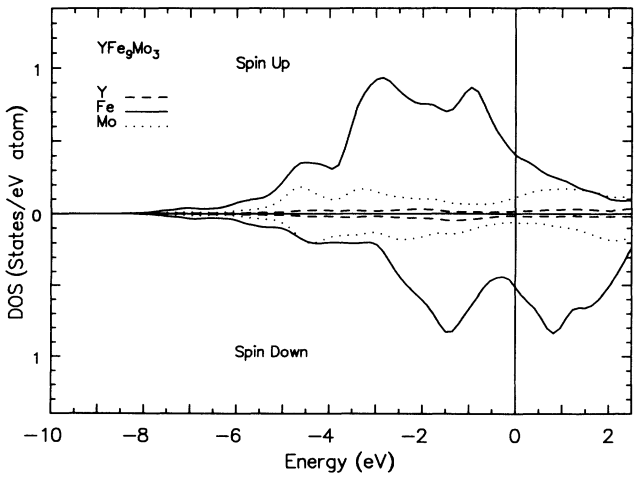

FIG. 3. Spin-polarized partial density of states for YFe_9Mo_3.

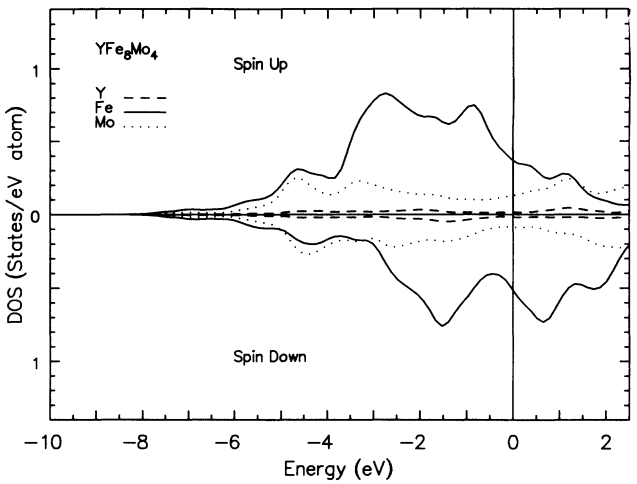

FIG. 4. Spin-polarized partial density of states for YFe_8Mo_4.

$$\bar{\delta}(\text{mm/sec}) = -0.131 - 0.032x \ .$$

The negative isomer shift means that we have an increase in the charge density of the s electrons at the iron nucleus. Previous measurements on $YFe_{12-x}V_x$ by Chunle *et al.*[12] and Cadogan *et al.*[15–17] also give negative isomer shifts.

Figure 8 shows the Mössbauer spectra and the fitting at $T=25$ K for $x=0.5$, 1, and 2. $\bar{H}_{hf}$ for $YFe_{10}Mo_2$ at $T=25$ K is 209 kOe which is close to the value of 230 kOe found by Denissen, Coehoorn, and Buschow[10] at $T=10$ K. The average isomer shift (Fig. 7) shows a linear decrease (solid line) with x according to the following equation:

$$\bar{\delta}(\text{mm/sec}) = -0.017 - 0.012x \ .$$

Samples with Mo concentrations $x=3$ and 4 were found to be paramagnetic at room temperature and magnetically ordered at low temperatures as seen in Figs. 9 and 10. The spectra at room temperature were fitted

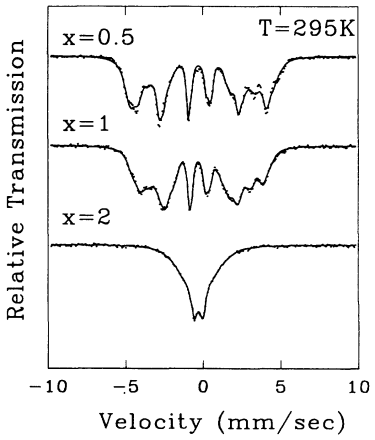

FIG. 5. Room-temperature Mössbauer spectra of $YFe_{12-x}Mo_x$ compounds. The solid curves represent the fitting.

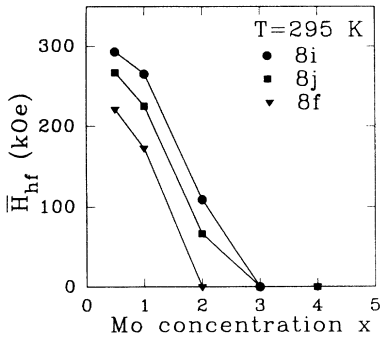

FIG. 6. The average hyperfine field for different Fe sites of $YFe_{12-x}Mo_x$ as a function of x.

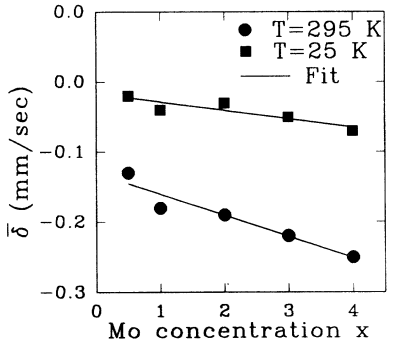

FIG. 7. The average isomer shift of $YFe_{12-x}Mo_x$ as a function of x at $T=295$ and 25 K. The solid lines represent the linear fitting.

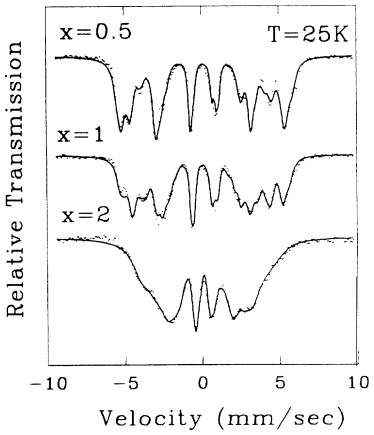

FIG. 8. Mössbauer spectra of $YFe_{12-x}Mo_x$ at $T=25$ K. The solid curves represent the fitting.

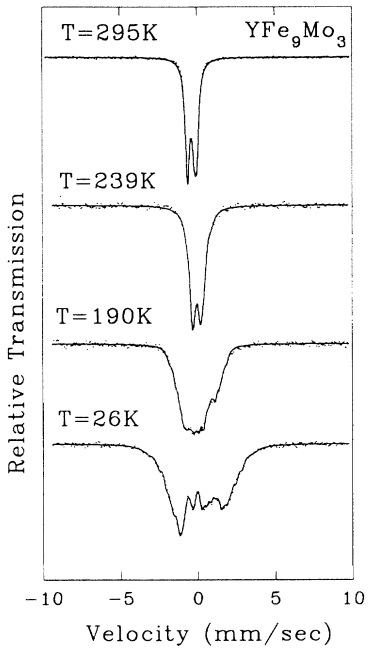

FIG. 9. Mössbauer spectra of YFe_9Mo_3 at different temperatures. The solid curves represent the fitting.

with two subspectra for $x=4$ and three for $x=3$. The low-temperature spectra were fitted with different components with the intensities given in Table I. The average hyperfine field for different sites was found to increase with increasing temperature as shown in Fig. 11. The average isomer shift was found to increase with decreasing temperature. This can be attributed to the second-

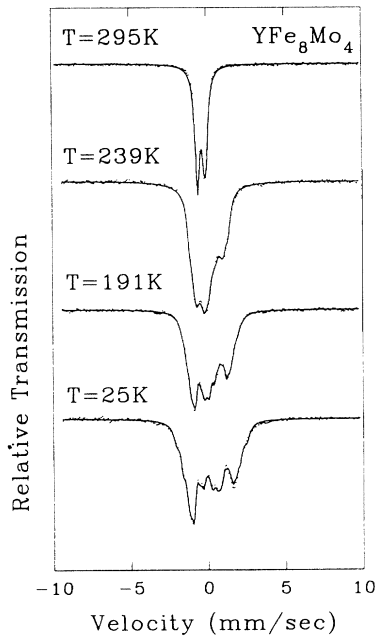

FIG. 10. Mössbauer spectra of YFe_8Mo_4 at different temperatures. The solid curves represent the fitting.

order Doppler shift (δ_R) which is defined as[25] $\delta_R=\delta(T)-\delta(RT)$. We find that δ_R depends on x and at $T=25$ K the dependence is given by $\delta_R=0.02+0.12x^{1/4}$.

The average H_{hf} at $T=25$ K for each site decreases with x (Fig. 12) which is in qualitative agreement with the calculated magnetic moments. The ratio of $\bar{H}_{hf}$ at 25 K to the calculated magnetic moment for different sites as a function of x is plotted in Fig. 13. The average value of the ratio at $x=1$ is 141 kOe/μ_B which is close to the α-Fe value. However, this value goes down with increasing x which presumably is due to the decrease in the number of near-neighbor Fe atoms. The sizable hyperfine field values for $x\geq 2$ samples along with the small high-field magnetization values is most reasonably explained by the noncollinearity of the magnetic moments, as discussed above.

The Mössbauer spectrum at $(H_{hf})_{max}<60$ kOe looks like a paramagnetic doublet due to quadrupole splitting. We used this criterion to estimate the magnetic ordering temperatures for $x=3$ and 4 samples. In Fig. 14, when $(H_{hf})_{max}=60$ kOe the Mössbauer magnetic ordering temperatures are about 240 and 274 K for $x=3$ and 4, respectively. $(H_{hf})_{max}$ for $x=4$ becomes higher than $(H_{hf})_{max}$ for $x=3$ at $T\approx 210$ K (Fig. 14). To explore this behavior further we did magnetization measurements for these two samples. We find that the field-cooled magnetization at 10 kOe applied field versus T has similar crossover around $T=230$ K as shown in Fig. 15. The results for low field ($H=100$ Oe) magnetic measurements for

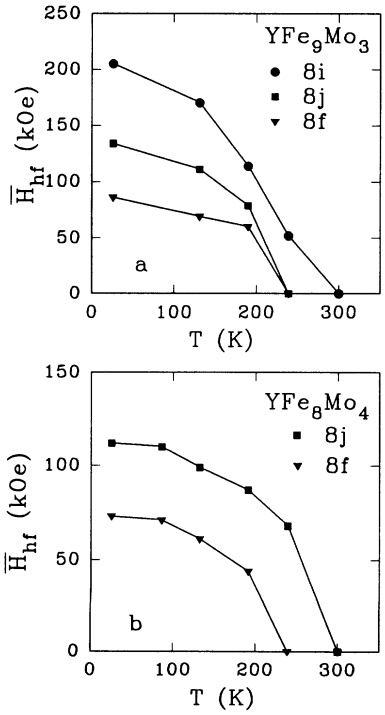

FIG. 11. Temperature dependence of the average hyperfine fields for different Fe sites of (a) YFe_9Mo_3 and (b) YFe_8Mo_4. The solid lines are drawn as a guide to the eye.

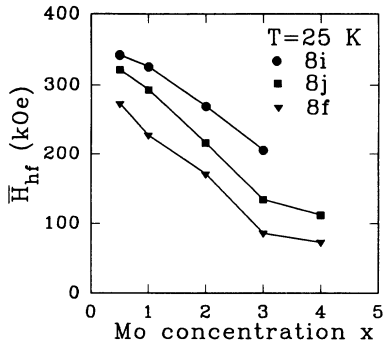

FIG. 12. The average hyperfine field for different Fe sites of $YFe_{12-x}Mo_x$ as a function of x.

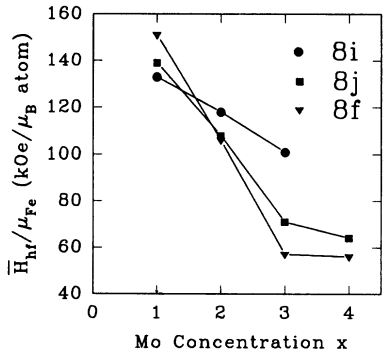

FIG. 13. The ratio of the average hyperfine field ($\bar{H}_{hf}$) at $T=25$ K to the calculated magnetic moment (μ) for different Fe sites as a function of x.

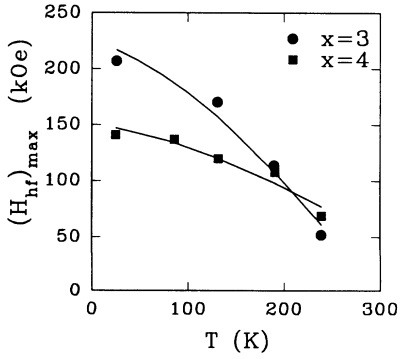

FIG. 14. Temperature dependence of the maximum hyperfine fields of YFe_9Mo_3 and YFe_8Mo_4. The solid lines are drawn as a guide to the eye.

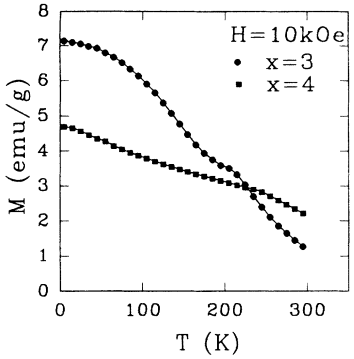

FIG. 15. Temperature dependence of the field-cooled magnetization of YFe_9Mo_3 and YFe_8Mo_4 at an applied field of 10 kOe.

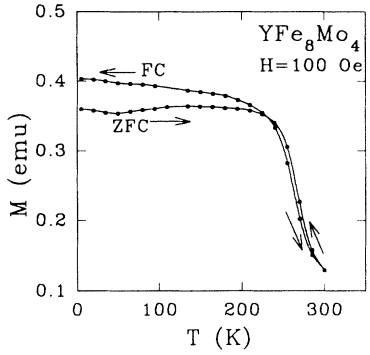

FIG. 17. Temperature dependence of zero-field-cooled (ZFC) and field-cooled (FC) magnetization for YFe_8Mo_4 at an applied field of 100 Oe.

$x=3$ and 4 are shown in Figs. 16 and 17, where the magnetic measurements on samples demagnetized at room temperature and cooled to 5 K in zero field [zero-field cooled (ZFC)] were made in a field of 100 Oe as the temperature was raised to 300 K. The temperature was then reduced to 5 K again with an applied field of 100 Oe, and M was measured with the same field [field cooled (FC)]. Low-field measurement for $x=3$ shows the existence of irreversible phenomenon as seen from the separation of the FC and ZFC curves (Fig. 16). This indicates that in the freezing process clusters of spins are involved, which is similar to spin-glass behavior. The ZFC peak is broad, which may be due to the existence of ferromagnetic clusters with different site moments and scattered orientations of the moments. Similar behavior has been observed by Christides *et al.*[23] for $x=2$ and by Angnostou *et al.*[24] for $x=1$ and 2. This behavior can be attributed to the disorder of the 8*i* sites which are partially occupied by Mo. YFe_8Mo_4 does not show this behavior (Fig. 17) which may be connected with the assumption that all the 8*i* sites are now mostly occupied by Mo. The coercivities of samples $x=3$ and 4 were found by measuring the hysteresis loops using AGFM with a maximum field of 10 kOe. Figure 18 shows that the coercivity for $x=3$ decreases with increasing temperature and it becomes very small at a temperature of 100 K which corresponds to the position of the peak of the ZFC. The coercivity for $x=4$ was negligible down to $T=30$ K. The coercivity results support the interpretation of the low-field magnetization measurements described above.

V. CONCLUSIONS

Magnetic properties of $YFe_{12-x}Mo_x$ have been studied by Mössbauer spectroscopy and magnetization measurements. Also spin-polarized electronic structure calculations have been carried out in the local-density approximation. Measurements at room temperature show that samples with $x=0.5$, 1, and 2 are ferromagnetic and $x=3$ and 4 are paramagnetic. All low-temperature Mössbauer data show that all the samples are magnetically ordered and the hyperfine fields decrease with increasing x in qualitative agreement with the calculated magnetic moments. The calculations, which simulate the disordered structure by a supercell method, predict that $YFe_{12-x}Mo_x$ for $x=1$, 2, 3, and 4 are ferromagnetically ordered. The experimental magnetization decreases more rapidly with increasing x that implied by the Mössbauer data and calculations. This disagreement most likely is due to an increase in the noncollinear arrangement of magnetic moments with increasing Mo concentrations, which is not considered in local-density calculations. To

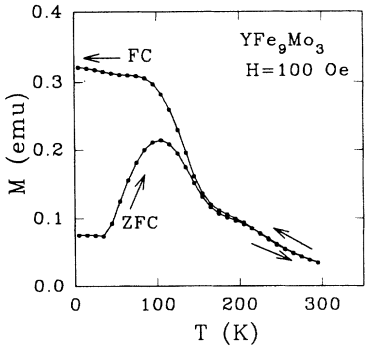

FIG. 16. Temperature dependence of zero-field-cooled (ZFC) and field-cooled (FC) magnetization for YFe_9Mo_3 at an applied field of 100 Oe.

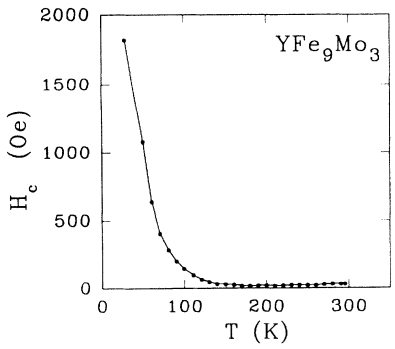

FIG. 18. Temperature dependence of the coercivity of YFe_9Mo_3.

explore this point further one must do Mössbauer measurements as a function of applied magnetic field. The low-field magnetization and coercivity measurements on YFe_9Mo_3 show spin-glass-like behavior, which also suggests the increase of some degree of antiferromagnetic coupling. This is similar to what has been observed by others for $YFe_{11}Mo$ and $YFe_{10}Mo_2$. However, we do not see this low-field behavior for YFe_8Mo_4. Since almost all the 8*i* sites are occupied by Mo for $x=4$, the atomic disorder for this sample is much smaller than that for $x=1$, 2, and 3. Thus, the frustration effects, which produce spin-glass-like or cluster-glass phenomena, seem to be related to atomic disorder at the 8*i* sites.

ACKNOWLEDGMENTS

We thank the United States Department of Energy for support under Grant No. DE-FG2-86ER45262, the National Science Foundation for support under Grant No. INT-9123488, and the Cornell National Supercomputing Facility which is supported by the NSF.

[1]D. B. De. Mooij and K. H. Buschow, J. Less-Common. Met. **136**, 207 (1988).
[2]K. H. J. Buschow, D. B. De Mooij, M. Brouha, H. H. A. Smit, and R. C. Thiel, IEEE Trans. Magn. **MAG-24**, 1161 (1988).
[3]J. Yang, S. Dong, Y. Yang, and B. Cheng, J. Appl. Phys. **75**, 3013 (1994).
[4]R. B. Helmholdt, J. J. M. Vleggaar, and K. H. J. Buschow, J. Less-Common Met. **138**, L11 (1988).
[5]Hong Sun, Y. Morii, H. Fujii, M. Akayama, and S. Funahashi, Phys. Rev. B **48**, 13 333 (1993).
[6]R. Coehoorn, Phys. Rev. B **41**, 11 790 (1990).
[7]A. S. Fernando, J. P. Woods, S. S. Jaswal, D. Welipitiya, B. M. Patterson, and D. J. Sellmyer, J. Appl. Phys. **75**, 6303 (1994).
[8]S. Ishida, S. Asano, and S. Fujii, Physica B **193**, 66 (1994).
[9]S. S. Jaswal, Y. G. Ren, and D. J. Sellmyer, J. Appl. Phys. **67**, 4564(1990); S. S. Jaswal, J. Appl. Phys. **69**, 5703 (1991); Phys. Rev. B **48**, 6156 (1993).
[10]C. J. M. Denissen, R. Coehoorn, and K. H. J. Buschow, J. Magn. Magn. Mater. **87**, 51 (1990).
[11]Th. Sinnemann, M. Rosenberg, and K. H. J. Buschow, J. Less-Common Met. **146**, 223 (1989).
[12]Y. Chunli, Z. Rongjie, L. Fashen, Z. Wending, and L. Jian, Chin. Phys. Lett. **7**, 373 (1990).
[13]Bo-Ping Hu, Hong-Shuo Li, J. P. Gavigan, and J. M. D. Coey, J. Phys. Condens. Matter **1**, 755 (1989).
[14]C. Christides, A. Kostikas, D. Niarchos, and A. Simopoulos, J. Phys. (Paris) Colloq. **49**, C8-539 (1988).
[15]J. M. Cadogan, J. Less-Common Met. **147**, L7 (1989).
[16]J. M. Cadogan, J. Alloys Compounds **177**, L25 (1991).
[17]J. M. Cadogan, J. Jing, and S. J. Campbell, Hyperfine Interact. **68**, 299 (1991).
[18]F. R. De Boor, Huang Ying-Kai, D. B. De Mooij, and K. H. J. Buschow, J. Less-Common Met. **135**, 199 (1987).
[19]Hong Sun, M. Akayama, K. Tatami, and H. Fujji, Physica B **183**, 33 (1993).
[20]K. Ohashi, Y. Tawara, R. Osugi, and M. Shimao, J. Appl. Phys. **64**, 5714 (1988).
[21]Y. Z. Wang, B. P. Hu, X. L. Rao, G. C. Liu, L. Song L. Yin, and W. Y. Lai, J. Appl. Phys. **75**, 6226 (1994).
[22]M. Jurczyk, J. Less-Common Met. **162**, 149 (1990).
[23]C. Christides, A. Kostikas, G Zanganelis, and V. Psycharis, Phys. Rev. B **47**, 11 220 (1993).
[24]M. Anagnostou, E. Devlin, V. Psycharis, A. Kostikas, and D. Niarchos, J. Magn. Magn. Mater. **131**, 157 (1994).
[25]*Advances in Mössbauer Spectroscopy,* edited by B. V. Thosar, P. R. Iyengar, J. K. Srivastava, and S. C. Bhargava (Elsevier Science, Amsterdam, 1983).